Broadband Polarizer Miter Bend for High-Power Radar Applications

Daniel Haas[1], Alexander Marek[1], Manfred Thumm[1,2], John Jelonnek[1,2], Matthias Jirousek[3] and Markus Peichl[3]

[1]IHM, [2]IHE, Karlsruhe Institute of Technology (KIT), Karlsruhe, Germany
[3]Microwaves and Radar Institute, German Aerospace Center (DLR), Oberpfaffenhofen, Germany
daniel.haas@kit.edu

Abstract — **Polarizer miter bends are used to alter the polarization in overmoded waveguides. For future space debris observation with broadband high power W-band radar sensors these are important transmission line components. A polarizer miter bend uses a grooved mirror as phase grid for polarization. The present paper addresses a suitable design of such a phase grid for broadband high power radar applications within the frequency range from $90\,\text{GHz}$ to $100\,\text{GHz}$. An appropriate parameter combination is found by a parametric study. For reduction of the required amount of calculation a plane wave approximation and unit cell simulations are used. With a suitable parameter combination a cross polarization of $X_{\text{pol}} \leq -26\,\text{dB}$ can be achieved within the considered frequency range. This corresponds to a suitable value for radar applications.**

Keywords — **Polarizer, Polarizer Miter Bend, Cross Polarization, High-Power Transmission Line, Unit Cell, Space Debris, Radar.**

I. INTRODUCTION

The amount of space debris in low earth orbit (LEO) is increasing rapidly [1]. Collisions with operating satellites can destroy critical infrastructure and therefore cause enormous damage [2, 3]. Space debris can be detected and mapped by high performance radar sensors [1, 4]. With those radar data the probability of collisions can be calculated and in case of doubt, necessary evasive maneuvers can be initiated. Of particular importance are imaging radar sensors [1, 3]. Those allow further conclusions about rotational axes and rotational speeds of larger space debris like unmanoeuvrable satellites [1]. Such additional informations allows even more accurate estimations of individual orbits [1, 3].

Due the enormous progress in the field of high power microwave technology, corresponding radar sensors can also be operated in high frequency bands such as the W-band [4]. Due to the high bandwidth available there, very high resolutions can be achieved [4, 5]. In near future even W-band transmission powers in the range of $100\,\text{kW}$ could be achieved [6]. To realize a W-band radar sensor with such a high transmission power as well a suitable high power amplifier as a suitable transmission line is required. The transmission line connects the output of the high power amplifier with the antenna feed. Due to the high power, overmoded transmission lines are required. A suitable transmission mode is the HE_{11} hybride mode. Low ohmic loss and small mode conversion can be achieved [7]. The HE_{11} mode is also the output mode of the proposed high power amplifier concept presented in [6].

For a functional radar system rotary joints are essential. These allow antenna movements in azimuth and elevation. However the polarization plane of a linearly polarized mode, like HE_{11}, is twisted by a rotary joint. To avoid such issues, the circularly polarized HE_{11} mode can be used for transmission.

For circular polarization a suitable polarizer is required. In nuclear fusion technology, polarizer miter bends are commonly used [8]. A miter bend allows the change of direction of a high-power transmission line by $90\,^\circ$ [9]. In the simplest case the fields are reflected at a plane mirror aligned by $45\,^\circ$. At a polarizer miter bend a phase grid is used instead of a plane mirror. The design of such a phase grid for broadband polarization is discussed in the present paper.

The paper is organized as follows: In section II formulas to calculate the cross polarization are derived. In section III fundamental aspects of a phase grid are introduced. The design of the phase grid is addressed in section IV. Section V closes with a conclusion of the considered aspects and the proposed design of the broadband polarizer miter bend.

II. CROSS POLARIZATION

For simplification a linearly polarized plane wave is assumed. The propagation direction shall be in $\vec{e}_z$−direction ($E_z = 0$). With an amplitude error ΔA and a phase error $\Delta \varphi$ follows:

$$E_x = \Delta A \cdot \sin(\omega t + \Delta \varphi)$$
$$E_y = \sin(\omega t) \tag{1}$$

The polarization errors lead to an elliptical polarization. In the ideal case applies: $\Delta A = 1$ and $\Delta \varphi = 0$.

The cross polarization is defined as the ratio of the time averaged signal power in the desired polarization plane and the time averaged signal power in the orthogonal polarization plane. Equation (1) describes a $45\,^\circ$ linearly polarized wave. To separate the orthogonal polarization planes an appropriate rotation matrix is used. This rotates the coordinate system by $45\,^\circ$:

$$\begin{pmatrix} E_{x'} \\ E_{y'} \end{pmatrix} = \begin{pmatrix} \cos(\pi/4) & \sin(\pi/4) \\ -\sin(\pi/4) & \cos(\pi/4) \end{pmatrix} \cdot \begin{pmatrix} E_x \\ E_y \end{pmatrix} \tag{2}$$

The cross polarization follows as:

$$X_{\text{pol}} = \frac{\langle E_{y'}{}^2 \rangle}{\langle E_{x'}{}^2 \rangle} \tag{3}$$

The inner product $\langle \bullet \rangle$ is defined for a power signal as [10]:

$$\langle \bullet \rangle = \lim_{T \to \infty} \frac{1}{T} \int_{-T/2}^{T/2} \bullet \; dt \qquad (4)$$

Equation (1), (2), (3) and (4) lead to:

$$X_{\text{pol}} = \frac{\Delta A^2 - 2\Delta A \cos(\Delta\varphi) + 1}{\Delta A^2 + 2\Delta A \cos(\Delta\varphi) + 1} \qquad (5)$$

For a known phase error $\Delta\varphi$ and amplitude error ΔA equation (5) can be used to calculate the present cross polarization. Fig. 1 shows a corresponding plot.
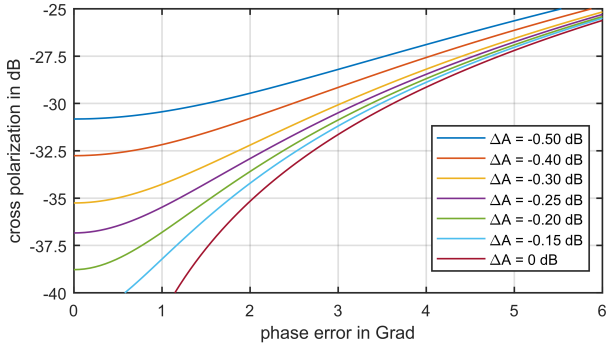

Fig. 1. Cross polarization in dB by varying phase error $\Delta\varphi$ and amplitude error ΔA.

III. FUNDAMENTAL ASPECTS

For circular polarization, orthogonal field components have to be phase shifted by $90\,°$ [11]. This can be achieved by a reflection grid: electrical field components parallel to the grid are reflected at the surface of the grid, electrical field components perpendicular to the grid penetrate into the grid and are reflected at the bottom. It results a time delay which can be used for polarization. Fig. 2 shows a simplified sketch of a rectangular reflection grid with the grid height h, grid period p and grid width a.
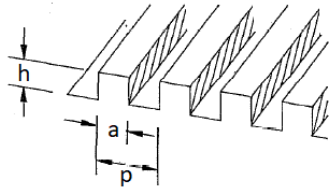

Fig. 2. Rectangular reflection grid with grid height h, grid period p and grid width a. (Figure based on [12])

In principle, at vertical wave incidence a grid height of $h_0 = \lambda/8$ and an alignment of $\psi = 45\,°$ is required for a phase shift by $90\,°$. The angle ψ refers to the polarization plane of the linearly polarized incident wave. According to [8], for an incidence under Θ applies:

$$h = \frac{h_0}{\cos(\Theta)} \qquad (6)$$

In fact, in the microwave range even electrical field components parallel to the grid are penetrating slightly into

the grid [13, 14]. Therefore, the required grid height has to be chosen slightly higher than expected from equation (6) [13].

For a too large grid period p the phase grid acts as a diffraction grid with multiple grading lobes [15]. To avoid this behavior the grid period has to fulfill [8]:

$$p < \frac{\lambda}{1 + \sin(\Theta)\cos(\psi)} \qquad (7)$$

With $\Theta, \psi = 45\,°$ follows: $p_{\max} \approx 0.67 \cdot \lambda$.

To avoid critical field strengths and electrical arc breakdowns curvature radii have to be used at sharp edges. Since the field components penetrates deeper / less deeper into the grid thereby [16], a reduced phase shift occurs. This effect has also to be considered by adjusting the grid height h.

IV. DESIGN

Following [17, 18], only at the top end of the grid curvature radii are taken into account. At the bottom of the grid no critical field strengths are expected. In [18] results of high power measurements at $110\,\text{GHz}$ and $900\,\text{kW}$ are presented with curvature radii of $R = 0.1\,\text{mm}$. The curvature radii of $R = 0.1\,\text{mm}$ shall be adopted to the present phase grid. No critical field strengths are expected thereby.

Further parameters are the grid width a and the grid period p. An appropriate parameter combination is determined by a parametric study. Section IV-A introduces the used principle approach. Section IV-B addresses the results of the parametric study.

A. Principle Approach

For simplification a plane wave approximation is used. For a waveguide diameter $D \geq 12 \cdot \lambda$ results of a plane wave approximation can be transfered to a HE_{11} wave [8]. Due to the plane wave approximation the phase grid can be modelled as an unit cell. That reduce the required calculation effort drastically. Now only a geometrical structur in the dimension of a few millimeters has to simulated. By introducing Floquet boundries [19] the simulation results of the unit cell can be transfered to an extended phase grid. This principle approch is common used for simulations of metamaterials and reflectarrays [19] and could transfered well to the present phase grid. Simulations were done with CST Microwave Studio. Fig. 3 shows the utilized simulation model.
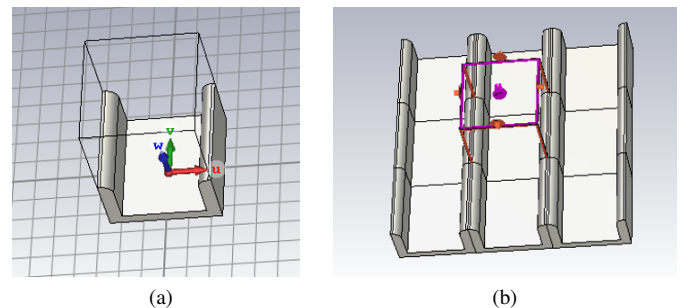

(a)   (b)

Fig. 3. CST-Model: (a) unit cell; (b) details of the extended phase grid due Floquet boundries.

For the parametric study the grid width a is varied between $0.25\,\text{mm}$ and $1.5\,\text{mm}$. The grid period p ist varied between $0.5\,\text{mm}$ and $1.75\,\text{mm}$. It is taken into account that the grid width a must not be too small for a practical realization. The grid period p have to fulfill equation (7).

For each parameter combination the phase history is simulated with N frequency points within the frequency range from $90\,\text{GHz}$ to $100\,\text{GHz}$. Then the rate of change $\partial\varphi/\partial f$ is calculated by numerical derivation and used for the evaluation function:

$$\Omega(a,p) = \frac{1}{N}\sum_{n=1}^{N}\left|\frac{\partial\varphi}{\partial f}\right| \qquad (8)$$

Each parameter combination results in a scalar value. That can be used as indicator of the reachable bandwidth. In the ideal case applies: $\Omega(a,p) = 0$.

It was found that the exact grid height has a minor impact to the reachable bandwidth. Therefore, equation (6) is still used to initialize the parametric study. The exact value of the grid height for the desired center frequency is chosen at the end of the procedure.

B. Results

Fig. 4 shows the values of the evaluation function and its gradient field in dependence of the grid width a and the grid period p. Each pixel represents a single simulation. In the white area there are no physically feasible parameter combinations.
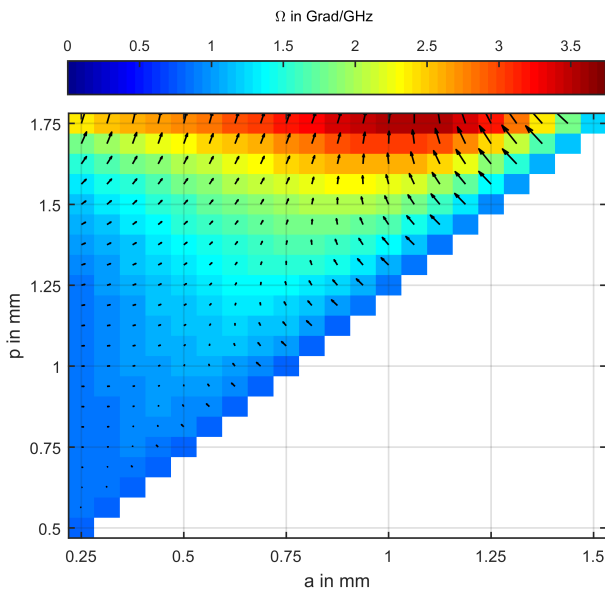

Fig. 4. Parametric study of a rectangular phase grid with grid width a and grid period p (small value $\hat{=}$ higher bandwidth, high value $\hat{=}$ smaller bandwidth). In black: corresponding gradient field.

It is shown that the frequency behavior depends strongly on the grid width a and the grid period p. As an appropriate parameter combination follows: $a = 0.25\,\text{mm}$ and $p = 1\,\text{mm}$. As well the value of the evaluation function as its gradient is low there. The latter is important to reduce the influence of

manufacturing tolerances by a practical realization. The grid height h is chosen to achieve an exact phase shift of $90°$ at the center frequency of $95\,\text{GHz}$. It results: $h = 0.48\,\text{mm}$.

Fig. 5 shows the resulting phase error $\Delta\varphi$ (in blue) and amplitude error ΔA (in brown) within the frequency range from $90\,\text{GHz}$ to $100\,\text{GHz}$. For comparison also results of a less suitable parameter combination are shown (see Fig. 4: $a = 1.06\,\text{mm}$, $p = 1.75\,\text{mm}$ and $h = 0.42\,\text{mm}$).
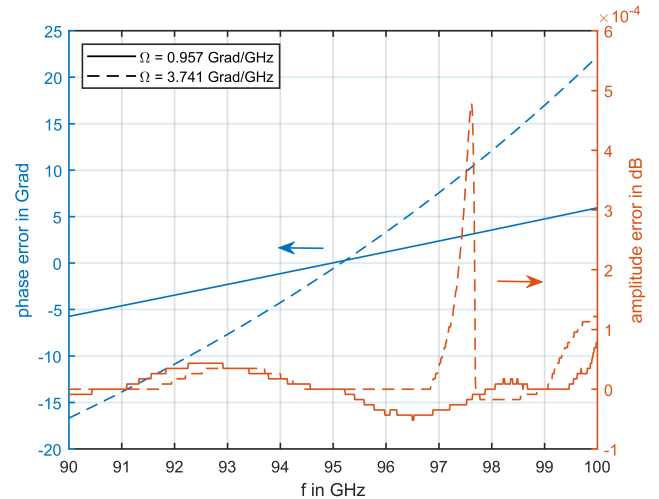

Fig. 5. Phase error $\Delta\varphi$ and amplitude error ΔA of a rectangular phase grid with suitable (solid curves) and less suitable (dashed curves) parameter combination.

It is shown that for a appropriate parameter combination the phase error $\Delta\varphi$ can be limited to $\pm 5.8°$. For a less suitable parameter combination the phase error is much higher. The amplitude error is always quite small. The small variations should be results of numerical uncertainties and can be neglected. Following $\Delta A = 1$ is assumed.

With equation (5), $|\Delta\varphi| \leq 5.8°$ and $\Delta A = 1$ follows: $X_{\text{pol}} \leq -25.91\,\text{dB}$. This corresponds to a suitable value for radar applications [20].

It has to be noted that the worst case value of $X_{\text{pol}} \approx -26\,\text{dB}$ occurs just at the frequency band edges at $90\,\text{GHz}$ and $100\,\text{GHz}$. Within the frequency range the cross polarization is even better. Fig. 6 shows a corresponding plot. The normalized signal power in the co (in blue) and cross (in brown) polarization within the frequency range from $90\,\text{GHz}$ to $100\,\text{GHz}$ is shown. For comparison also results of a less suitable parameter combination are shown (see Fig. 4: $a = 1.06\,\text{mm}$, $p = 1.75\,\text{mm}$ and $h = 0.42\,\text{mm}$). The co polarization is calculated by:

$$C_{\text{pol}} = 1 - X_{\text{pol}} \qquad (9)$$

It is shown that the polarization purity depends strongly on the parameter combination of the grid width a and the grid period p. For an unsuitable parameter combination the cross polarization is up to $11\,\text{dB}$ worse than for a suitable parameter combination. Due cross polarization loss of signal power in the desired polarization plane occurs. Fig. 6 shows that for

an unsuitable parameter combination these losses reach nearly $4\,\%$. For a suitable parameter combination the polarization loss is just close to $0.25\,\%$. Again it is shown that a suitable design of the phase grid is essential.
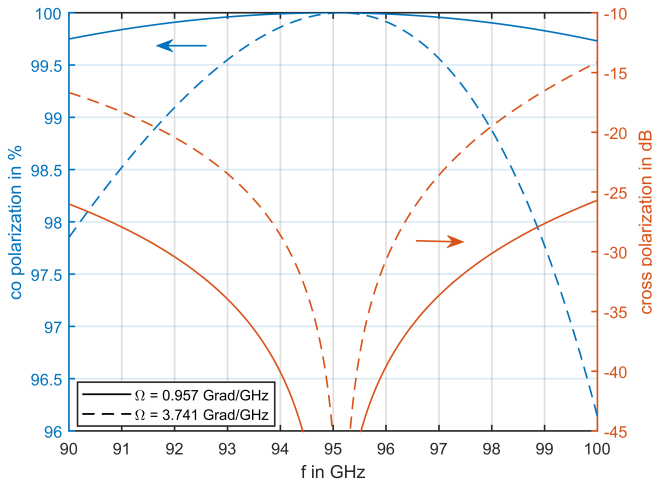

Fig. 6. Co and cross polarization by a suitable (solid curves) and less suitable (dashed curves) parameter combination.

The presented approach to design a broadband polarizer miter bend could be transferred to numerous further applications. In addition, sinusoidal- or triangle-shaped reflection grid profiles or even more optimized corrugation contours could be studied. The required computational effort is always quite small thereby.

V. Conclusion

The present paper addresses a broadband polarizer miter bend for high-power radar applications. For future space debris observation with broadband high-power W-Band radar sensors, a polarizer miter bend is an important transmission line component.

For a suitable parameter combination a parametric study was done. To reduce the required amount of calculation a plane wave approximation and unit cell simulations were used. Within the frequency band from $90\,\mathrm{GHz}$ to $100\,\mathrm{GHz}$ a cross polarization of $X_{\mathrm{pol}} \leq -26\,\mathrm{dB}$ could be achieved. This corresponds to a suitable value for radar applications. For an unsuitable parameter combination the cross polarization is much higher.

Further research activities shall address the mode purity and the exact mode content at the output of the polarizer miter bend. It is known that mode conversion occurs in miter bends due to diffraction [9, 21]. This also applies to polarizer miter bends. The amount of mode conversion loss of the HE_{11} mode can be estimated quite accurately [9]. For radar applications also the exact mode content is important. Spurious modes could impair the cross polarization or the sidelobe level of the radar antenna. For high performance radar sensors these effects have to be taken into account.

References

[1] D. Mehrholz et al. "Detecting, Tracking and Imaging Space Debris". In: *ESA Bulletin 109* (2002).

[2] M. Williamson. "Space Junk makes an Impact". In: *IEE Review, Vol. 52, No. 1* (2006).

[3] J. Ender et al. "Radar techniques for space situational awareness". In: *International Radar Symposium* (2011).

[4] M. Czerwinski and J. Usoff. "Development of the Haystack Ultrawideband Satellite Imaging Radar". In: *Lincoln Laboratory Journal, Vol. 21, No. 1* (2014).

[5] J. Eshbaugh et al. "HUSIR Signal Processing". In: *Lincoln Laboratory Journal, Vol. 21, No. 1* (2014).

[6] S. Samsonov et al. "Cascade of Two W-Band Helical-Waveguide Gyro-TWTs With High Gain and Output Power: Concept and Modeling". In: *IEEE Transaction on Electron Devices, Vol. 64, No. 3* (2017).

[7] J. Doane. "Propagation and Mode Coupling in Corrugated and Smooth-Wall Circular Waveguides". In: *Infrared and Millimeter Waves, Vol. 13, Ch. 5* (1985).

[8] J. Doane. "Grating Polarizers in Waveguide Miter Bends". In: *International Journal of Infrared and Millimeter Waves, Vol. 13, No. 11* (1992).

[9] J. Doane and C. Moeller. "HE11 mitre bends and gaps in a circular corrugated waveguide". In: *International Journal of Electronics, Vol. 77, No. 4* (1994).

[10] F. Puente and U. Kiencke. *Messtechnik: Systemtheorie für Ingenieure und Informatiker*. Springer, 2011.

[11] C. Balanis. *Antenna Theory: Analysis and Design, Third Edition*. Wiley-Interscience, 2005.

[12] K. Nagasaki, A. Isayama, and A. Ejiri. "Application of a grating polarizer to the 106.4 GHz ECH system on Heliotron-E". In: *Review of Scientific Instruments, Vol. 66, No. 6* (1995).

[13] Y. Kok and N. Gallagher. "Relative phases of electromagnetic waves diffracted by a perfectly conducting rectangular-grooved grating". In: *Journal of the Optical Society of America A, Vol. 5, No. 1* (1988).

[14] R. Kastner. "A Spectral-Iteration Technique for Analyzing a Corrugated-Surface Twist Polarizer for Scanning Reflector Antennas". In: *IEEE Transaction on Antennas and Propagation, Vol. 30, No. 4* (1982).

[15] F. Pedrotti et al. *Optik für Ingenieure: Grundlagen*. Springer-Verlag, 2005.

[16] K. Nagasaki et al. "Polarizer with Nonrectangular Grooves in the HE11 Mode Transmission Line". In: *International Journal of Infrared and Millimeter Waves, Vol. 20, No. 5* (1999).

[17] T. Tsujimura et al. "Optimized design of polarizers with low ohmic loss and any polarization state for the 28 GHz QUEST ECH/ECCD system". In: *Fusion Engineering and Design, Vol. 114* (2017).

[18] N. Horie et al. "High power test of wideband polarizer for electron cyclotron current driving system in JT-60SA". In: *Fusion Engineering and Design, Vol. 122* (2017).

[19] M. Jayawardene and Y. Vardaxoglou. *3-D EM Simulation of Infinitive Periodic Arrays and Finite Frequency Selective Horns*. 2006.

[20] R. Touzi, P. Vachon, and J. Wolfe. "Requirement on Antenna Cross-Polarization Isolation for the Operational Use of C-Band SAR Constellations in Maritime Surveillance". In: *IEEE Geoscience and Remote Sensing, Vol. 7, No. 4* (2010).

[21] B. Katsenelenbaum. "Diffraction on plane mirror in broad waveguide junction". In: *Radio Engineering and Electronic Physics, 8* (1963).